Research Square

Preprints are preliminary reports that have not undergone peer review.
They should not be considered conclusive, used to inform clinical practice,
or referenced by the media as validated information.

Simultaneous transcranial electrical and magnetic stimulation boost gamma oscillations in the dorsolateral prefrontal cortex

Michele Maiella
Santa Lucia Foundation IRCCS
Elias Paolo Casula
Santa Lucia Foundation IRCCS
Ilaria Borghi
Santa Lucia Foundation IRCCS
Martina Assogna
Santa Lucia Foundation IRCCS
Alessia D'Acunto
Santa Lucia Foundation IRCCS
Valentina Pezzopane
Santa Lucia Foundation IRCCS
Lucia Mencarelli
Santa Lucia Foundation IRCCS
Maria Concetta Pellicciari
Santa Lucia Foundation IRCCS
Giacomo Koch (g.koch@hsantalucia.it)
Santa Lucia Foundation IRCCS

Article

Keywords: Transcranial alternated current stimulation, Transcranial magnetic stimulation, Dorsolateral prefrontal cortex, Gamma oscillations

Posted Date: April 19th, 2022

DOI: https://doi.org/10.21203/rs.3.rs-1550621/v1

License: This work is licensed under a Creative Commons Attribution 4.0 International License.
Read Full License

Abstract

Neural oscillations in the gamma frequency band have been identified as a fundament for synaptic plasticity dynamics and its alterations are central in various psychiatric and neurological conditions. Transcranial magnetic stimulation and alternating electrical stimulation may have a strong therapeutic potential by promoting gamma oscillations and plasticity. Here we applied intermittent theta-burst stimulation (iTBS), an established TMS protocol known to induce cortical plasticity, simultaneously with transcranial alternating current stimulation (tACS) at either theta (θtACS) or gamma (γtACS) frequency on the dorsolateral prefrontal cortex (DLPFC). We used TMS in combination with electroencephalography (EEG) to evaluate changes in cortical activity on both left/right DLPFC and over the vertex. We found that simultaneous iTBS with γtACS but not with θtACS resulted in an enhancement of spectral gamma power, a shift of individual peak frequency towards faster oscillations and an increase of local connectivity in the gamma band. These results were specific to the DLPFC and confined locally to the site of stimulation, not being detectable in the contralateral DLPFC. We argue that the results described here could promote a new and effective method able to induce long-lasting changes in brain plasticity useful to be clinically applied to several psychiatric and neurological conditions.

Introduction

During the last decades, a growing body of neurophysiological studies has focused on the possibility to interfere with and modulating neural oscillations. Cortical oscillatory activity represents the rhythmic activity of a population of neurons within a given frequency band [1], is crucial for brain networks dynamics [2,3] and underlies cognitive processes in healthy [4] and pathological brains [5]. Gamma oscillations in the prefrontal areas are involved in several cognitive functions including attention and memory [6,7]. Furthermore, several studies in human and animal models have suggested a role for γ oscillations in inducing and supporting synaptic plasticity mechanisms in cortical prefrontal [8] and motor areas [9].

Non-invasive brain stimulation (NIBS) techniques have been widely used to induce plastic changes in cortical areas, to modulate brain rhythms and influence the ongoing cortical activity. Intermittent theta-burst stimulation (iTBS) is a form of repetitive transcranial magnetic stimulation (rTMS) method, which consists of bursts of high-frequency stimulation (3 pulses at 50 Hz) repeated at intervals of 200 ms, that can induce robust long-lasting changes in the stimulated area [10]. It was firstly developed in animal models to mimic the natural patterns that support synaptic long-term potentiation (LTP) mechanisms [11,12]. iTBS has been successfully employed in the clinical ground in several conditions ranging from depression [13] to stroke recovery [14].

These iTBS after-effects seem to be mediated by GABAergic interneurons activity, which is also crucial for oscillatory activity modulation [15–17].

Transcranial alternating current stimulation (tACS) is another NIBS protocol delivering electrical stimulation with a sinusoid alternated current within a specific frequency. tACS can entrain ongoing brain oscillations activity and modulate brain areas in a frequency-dependent manner [18]. γtACS has been shown capable to interact with γ oscillatory activity in the motor cortex (M1) [19,20] as well as in the prefrontal cortex [21]. Moreover, tACS gained attention given the therapeutic potential to induce long-lasting increases of gamma oscillations, since a decrease in gamma activity is central in various psychiatric and neurological conditions such as schizophrenia [22] and Alzheimer's disease [23]. However, the therapeutic effect of NIBS protocols acting on gamma oscillations is currently limited by the fact that the after-effects are often variable, of small magnitude, and short-lasting [24].

Recently the pioneering work of Guerra and others showed that contemporary electrical and magnetic stimulation can promote robust after-effects on cortical oscillations when applied over M1 [25–27]. This combination has not been assessed in areas involved in cognitive functions such as the dorsolateral prefrontal cortex (DLPFC) which is involved in the pathophysiology of a wide range of neurological diseases [28–31].

Here, we used a novel approach by combining transcranial magnetic stimulation (TMS) and electroencephalography (EEG) to assess the potential after-effects of simultaneous iTBS and tACS on DLPFC cortical activity [32]. [33,34].

We hypothesize that entraining γ frequency by tACS during iTBS could boost the long-lasting plasticity after-effects of iTBS on oscillatory activity by inducing a synergistic effect on the underlying local networks.

Results

All 13 participants completed successfully the three-session protocol planned. The different stimulation protocols were all well-tolerated, and subjects reported no side effects. Single-pulse TMS evoked on EEG signal a well-known sequence of positive and negative deflections with amplitude ranging from − 3 to 3 μV and lasting up to ~ 250 ms (Fig. 1, Fig. 2). TMS-evoked cortical reactivity (panel (a)) last around 150 ms and it is characterized by a series of peaks such as P1 from 15 to 25 ms, P2 from 26 to 47 ms, P3 from 48 to 65 ms, P4 from 66 to 75 ms, P5 from 76 to 115 ms, P6 from 116 to 145 ms. This temporal dynamic, in terms of waveform and amplitude, looks similar for all the sites at baseline. The three peaks were detectable over all the three stimulated areas as expected (Veniero et al., 2013, Rosanova et al., 2009; Casula et al., 2016). No differences in the general amplitude are detected between DLPFC and Vertex ($p > .05$). In the first two peaks window (i.e. 15–60 ms after TMS) a dipole was focused over the stimulated area; from ~ 65 to ~ 120 ms after TMS spread negativity observable over both the hemispheres, followed by a strong positivity centred over the frontocentral electrodes, ranging from ~ 120 to ~ 250 ms after TMS. Figures 1,2 and 3 show the TMS-evoked potential (TEPs) over the different stimulation sites (l-DLPFC; r-DLPFC; vertex) in "tACS" and "Time" conditions. iTBS + γtACS stimulation showed a neuromodulation effect evident on the third peak while stimulating l-DLPFC (Fig. 1, panel (a)).

Figure 1 (b) depict the peaks analysis revealing a significant ANOVA “tACS” (γ, θ, sham) x “time” (T0, T1, T2) interaction [$F(10, 120) = 1.066$; $p = 0.05.$; $\eta^2 = .082$]. Post-hoc analysis showed that in the iTBS + γtACS stimulation condition the third peak significantly differed in t0 vs t1 times conditions ($p = 0.05$). No effects were found for r-DLPFC (Fig. 2) and vertex (Fig. 3) sites.

Figures 4, 5, and 6 show local TMS-evoked cortical oscillations. In detail, the figures represent the local oscillatory activity (Fig. 4l- DLPFC; Fig. 5r- DLPFC; Fig. 6 vertex). As depicted in panel (a), TMS-evoked cortical oscillations have similar baseline activity patterns characterized by a remarkable activation around 50 ms after TMS pulse in the frequencies between 20 to 30 Hz. A second activation can be identified from around 50 ms to 250 ms in lower frequencies such as approximately 6 Hz to 10 Hz. Cortical maps show the topographical cortical oscillations activation, which was stronger in areas around the stimulated site. Panel (b) represents the most expressed individual frequencies for all the stimulation conditions and during time. In baseline for all the conditions and areas, the most expressed individual frequencies were in a range between 22 Hz to 28 Hz. Figure 4 shows l- DLPFC cortical oscillations patterns dynamics before and after iTBS + tACS stimulation. We analyzed gamma oscillation (mean 30–50 Hz) power and individual frequency shifting in time. Gamma oscillation power analysis shows a significant difference between conditions (“Time”, “tACS”) [$F(4, 48) = 2.801$; $p = .03$; $\eta^2 = .189$]; post-hoc analysis reveals that iTBS + γtACS increase power in time between t0 vs t2 [$p = .05$]. No effects were originated by the other “tACS” conditions (iTBS + θtACS /sham tACS). A latter analysis was focused on the individual frequency shifting right after the iTBS + tACS stimulation; iTBS + γtACS stimulation modulates spectral shifting in the most expressed individual frequency [$F(2, 24) = 3.335$; $p = .05$; $\eta^2 = .217$]; post-hoc analysis reveal the difference between T0 vs T1 “Time” conditions [$p = .04$]. iTBS + θtACS /sham tACS stimulation conditions have no effects on individual frequency shifting. Figure 4 panel (b) shows these effects. No significant effects were reported for the same analysis in r- DLPFC and vertex (Figs. 5 and 6, panel (b)).

Figure 7 shows the individual frequency wavelet phase-locking value analysis (W-PLV). W-PLV was conducted on the data collected during l-DLPFC TMS-EEG recordings between F3-F5 and F3-F4 before and after iTBS + tACS stimulation for the three “tACS” conditions. Panel (a) represents W-PLV in F3-F5 and F3-F2 channels pairs for the “tACS” conditions in time. PLV values are higher in T0 for lower frequency bands and in a range between 22 to 28 Hz for both couples of electrodes. Figure 7 panel (b) represents histograms that show the neuromodulation iTBS + γtACS stimulation effects on W-PLV in l-DLPFC during time (T0; T1; T2) for a mean Gamma band range (30–50 Hz). W-PLV analysis shows a significant difference between conditions (“Electrode”, “Time”) [$F(2, 22) = 20.817$; $p = .01$; $\eta^2 = .654$] for the Gamma frequency (mean between 30–50 Hz); post-hoc analysis shows significant difference between T0 and T1 [F5 $p = .05$; F2 $p = .01$] and T0 and T2 [F5 $p = .004$; F2 $p = .002$] for both the F3-F5 and the F3-F2 pairs. These effects are depicted respectively in panel (b)’s left (F3-F5) and right (F3-F2) side histograms. No significant effects were reported for the same analysis in r- DLPFC and vertex.

Discussion

Here we show that simultaneous transcranial electrical and magnetic stimulation exerts a robust long-lasting increase in gamma oscillations in the DLPFC. We found that combined DLPFC iTBS-γtACS resulted in an enhancement of spectral gamma power, a shift of individual peak frequency towards faster oscillations, and in an increase of local connectivity in the gamma band. These results were specific to the stimulated area and confined locally to the site of stimulation, not being detectable in the contralateral DLPFC. This study aimed to take advantage of the iTBS and tACS properties to boost the capability that these two NIBS methods have to produce long-lasting oscillatory brain changes on DLPFC and to evaluate whether a synergistic effect would arise from this combination. Although there is great interest in the application of TBS in several neurological and psychiatric disorders, its clinical impact is somewhat limited by the variability of after-effects that have been reported in healthy studies evaluating the effects on the amplitude of the MEP. These studies showed that only approximately 50% of subjects undergoing iTBS show the expected significant motor MEP long-lasting increase [35–38]. Inter-subject variability is considered the most relevant limitation of non-invasive brain stimulation [39,40] since it affects the effectiveness of neuromodulation techniques and limits their clinical applications. Moreover, the magnitude of increase in MEPs amplitude after M1 iTBS and in TEPs amplitude after DLPFC iTBS is in the range of 20–50% as compared to baseline, again potentially limiting the clinical impact of this plasticity inducing protocol [41]. While initially iTBS was thought to produce more powerful and reproducible effects than other rTMS methods, a claim that has not been fully confirmed, its main attraction still relies on the speed of application with protocols lasting a few hundreds of seconds instead of several minutes [41]. Indeed iTBS through the high-frequency neuronal activation modulates cortical inhibition and GABA-ergic synaptic transmission, resulting in an enhancement of γ band expression [42]. iTBS is thought to activate Ca2 + influx to the postsynaptic neuron. The property, including the amount and the rate of the increase, determines the amount of the build-up of subsequent facilitation processes that modify the synaptic strength [43]. This notion is supported by animal studies showing that dysfunction of Inositol 1,4,5-trisphosphate receptors (InsP3Rs) that is required for LTP results in a conversion of LTD to LTP, while partial blockade of NMDARs to reduce the rate of Ca2 + influx results in a conversion of LTP to LTD [44].

On the other hand, tACS is a relatively new technique that can effectively modulate oscillatory brain activity through weak external alternating current at specific frequencies [18]. This effect is supported by research in animals [45] suggests that TES in phase with network-induced patterns can enhance neuronal discharge activity. Through the mechanism of stochastic resonance [46,47], the electric field, which in itself may be subthreshold, can be effectively summed with otherwise subthreshold effects of network-induced membrane voltage fluctuations, and the combined effect can generate spikes in a fraction of the neuronal population. However, there is still a lack of understanding about the exact mechanisms that modulate cortical activity as a function of tACS administration.

We argue that the robust synergistic effects observed here are the consequence of the interplay among gamma oscillations and the formation of cortical plasticity. The role of gamma activity in synaptic plasticity has been then confirmed throughout the last two decades by numerous investigations using

electrophysiological recordings in animals [48] and humans [49]. Although the exact physiological mechanism is still a matter of debate, it has been suggested that local inhibitory interneurons play a key role in synchronizing gamma oscillations among large neuronal populations [50–53]. Thus, when depolarized, local interneuron populations tend to generate synchronized inhibitory postsynaptic potentials in thousands of cells, inducing an entraining in fast gamma oscillations not only in local but also in distant neurons [33,51,54,55]. This is relevant since gamma-frequency synchronization between the activity of distant neuronal cells has emerged as a marker of connectivity within large cortical networks, during learning or memory processing [56,57]. During the formation of plasticity, an increase in gamma-activity coherence represents enhanced connectivity between distant neuronal populations in forming a new memory [58]. This latter element is particularly relevant since cognitive dysfunction in AD has been recently linked to a disorder of gamma oscillations [23]. In AD animal models, local changes in gamma oscillatory activity affect multiple brain centres critical for learning and memory, and other higher-order brain functions, such as the hippocampus and the prefrontal cortex [59–63]. Hence we believe that our current findings may have broad implications for treating gamma dysregulation in neurodegenerative disorders such as AD.

While we found that combined iTBS-γtACS induced robust after-effect on DLPFC cortical activity both in terms of excitability and oscillations, combined iTBS-θtACS did not result in any significant change. This finding is in line with the pioneering work of Guerra and colleagues showing that tACS delivered at lower frequencies in the alpha band leaves the iTBS-related LTP-like plasticity unchanged (Guerra et al., 2018, 2019).

In the current study, we adopted a protocol for combined stimulation of tACS and iTBS based on a synchronous start triggered externally. This approach is supposed to drive oscillatory activity using tACS while iTBS exerts its effects on local LTP-like mechanisms. However, other approaches are trying to apply controllable phase-synchronized rTMS with tACS to induce and stabilize neuro-oscillatory resting-state activity at targeted frequencies. For instance, Hosseinian and coll. [64] used a novel circuit to precisely synchronize rTMS pulses with the phase of tACS in the bilateral prefrontal cortex (PFC). They found that 10-Hz resting-state PFC power increased significantly with peak-synchronized rTMS + tACS, while rTMS timed to the negative tACS trough did not induce local or global changes in oscillations. Moreover, they also developed a novel stimulation protocol, where a single circuit precisely synchronizes rTMS pulses with the phase of tACS in the theta frequency band [65]. Similarly, Zrenner et al., [66] hypothesized that triggering TMS synchronized with the negative peak of endogenous alpha oscillations in left DLPFC would more effectively increase cortical excitability (as measured with TMS-evoked potentials) than a non-alpha-synchronized stimulation protocol.

The study has some limitations. Some control conditions such as theta-tACS alone and gamma-tACS alone are lacking. However, it has been shown previously that a few seconds of tACS are not supposed to exert any after-effect (Lafleur et al., 2021) and thus we did not weigh down our experimental procedure that was already quite demanding for the healthy subjects recruited for the study. The TMS-EEG

measurements did not include a sham stimulation condition to control for peripherally evoked potentials and muscle artefacts. In this regard, we adopted all the TMS that can result in non-specific effects, such as auditory and somatosensory stimulation that can affect the EEG response (Rocchi et al., 2021). We adopted several methodological precautions to avoid these artefacts. To reduce the auditory response, we used an ad-hoc masking noise; to reduce bone conduction of the TMS click and scalp sensation caused by coil vibration we placed a 0.5 cm foam layer underneath the coil. Finally, while our evidence seems to suggest that the synchronization of rTMS with peak oscillatory activity may have an impact on subsequent plasticity induction, this approach is technically limited to lower frequency bands in the theta-alpha range. Current methodological restraints do not allow to transfer of a similar approach towards higher frequencies such as those used in the gamma band in our case (70 Hz) since these cannot be reliably detected online with non-invasive scalp EEG recordings. Such hypothesis however could be tested in the future in patients with implanted electrodes.

In conclusion, we argue that the results described here could promote a new and effective method able to induce long-lasting changes in brain plasticity and connectivity, useful to be clinically applied to several psychiatric and neurological conditions.

Methods

Participants and procedure

13 healthy participants were enrolled in the study. Experimental within-subject design included three different randomized sessions every participant underwent to: (1) iTBS + γtACS stimulation; (2) iTBS + θtACS stimulation; (3) iTBS + sham tACS stimulation. During every session subject underwent TMS-EEG neurophysiological assessment on three testing times: before (T0) iTBS + tACS stimulation, 0 min (T1) and 20 min (T2) after the iTBS + tACS stimulation. Three cortical areas were studied using TMS-EEG: left dorsolateral prefrontal cortex (l-DLPFC), right dorsolateral prefrontal cortex (r- DLPFC) and vertex (Fig. 8). The study was approved by the local ethics committee (Ethical Committee Fondazione Santa Lucia, Via Ardeatina 306, 00179 Roma; Prot. CE/PROG.811; 19/02/2021)TMS-safety guidelines and medical regulations were fully followed by experimenters and written informed consent was obtained from each participant.

iTBS + tACS stimulation

The iTBS + tACS stimulation was applied over l- DLPFC and last for 190s, with the tACS electrode on the scalp and the iTBS coil just above it. A figure-of-eight coil with a diameter of 70 mm was used to deliver iTBS over the scalp site corresponding to the l- DLPFC (F3, according to 10–20 system). A MagStim Super Rapid magnetic stimulator (Magstim Company, Whitland, Wales, UK) was used to deliver the biphasic waveform pulse, with a pulse width of ∼0.1 ms. iTBS consist of a 2 seconds train of TBS that is repeated 20 times, every 10 seconds for a total of 190 seconds (600 pulses). Stimulation intensity was set at 80% of the active motor threshold (AMT), defined as the lowest intensity able to produce MEPs <

200 μV in at least five out of ten trials when the subject performed a 10% of maximum contraction using visual feedback [67]. AMT was tested over the motor cortex of the hemisphere target of the iTBS stimulation (i.e. left) with the same stimulation condition, such as with the tACS electrode behind the coil. Electromyographic activity was recorded from the contralateral FDI muscle, using two Ag-AgCl surface cup electrodes (9 mm) in a belly-tendon montage. Responses were amplified through a Digitimer D360 amplifier (Digitimer Ltd, Welwyn Garden City, Hertfordshire, UK): filters were set at 20 Hz and 2 kHz, with a sampling rate of 5 kHz; they were then recorded by a computer using SIGNAL software (Cambridge Electronic Devices, Cambridge, UK). During stimulation, the coil was oriented 45° with respect to l- DLPFC. A neuronavigation system (SofTaxic; E.M. S., Bologna s.r.l.) coupled with a Polaris Vicra infrared camera was used to ensure that in each subject iTBS was applied over the same spot across different sessions. Indeed stimulation point was set and memorized during the first session and imported at the beginning of the other two sessions, to make sure the stimulated area was constant across sessions. A Brainstim multifunctional system for low-intensity transcranial electrical stimulation (E.M. S., Bologna s.r.l.) was used to deliver the current stimulation using saline-soaked sponge electrodes (7 × 5 cm^2). The active electrode (anode) was placed on the scalp over the left- DLPFC (l- DLPFC, F3) and the reference (cathode) over the right deltoid muscle. During real stimulations, the current was set to 1 mA and delivered for 190s. No ramp-up and no ramp down were programmed for the stimulation. For the sham condition, the electric current was not applied, but there were a 2 seconds 1 mA ramp up and 2 seconds 1 mA ramp down, to give the subject real stimulation feelings. For γtACS the sinusoid frequency wave was set at 70 Hz; for θtACS, the sinusoid frequency wave was set at 5 Hz. iTBS and tACS were synchronized using a BrainTrigger (E.M. S., Bologna s.r.l.) and SIGNAL Software: both stimulations started exactly at the same time.

TMS-EEG cortical assessment

During every session, participants underwent an electroencephalographic (EEG) recording of a series of TMS pulses delivered in specific areas of interest. Consequently, it was possible to evaluate cortical reactivity, connectivity and plasticity during time. TMS was carried out using a Magstim R^2 stimulator with a 50 mm figure-of-eight coil (Magstim Company, Whitland, Wales, UK), which produces a biphasic waveform with a pulse width of ∼0.1 ms. TMS pulses were applied over the l- DLPFC, right- DLPFC (r- DLPFC) and vertex. According to scientific literature, the coil was differently oriented with respect to the mid-sagittal axis of the subject's head for each stimulation site: 45° over l- DLPFC and r- DLPFC, and parallel over the vertex, with the handle pointing backwards. The intensity of stimulation of single-pulse TMS was set at 110% of the resting motor threshold (RMT), defined as the lowest intensity producing MEPs of > 50 μV in at least five out of 10 trials in the relaxed first dorsal interosseous (FDI) muscle of the right hand [68]. The coil position was constantly monitored using a neuronavigation system (SofTaxic; E.M. S., Bologna s.r.l.), to ensure a high degree of reproducibility within the same session and across different sessions. Stimulation points were set and memorized at the beginning of the first session and imported at the beginning of the other two sessions, to make sure the stimulated areas were constant across times and sessions.

A TMS-compatible DC amplifier (BrainAmp, Brain Products GmbH, Munich, Germany) was used to record EEG activity from the scalp. The EEG was continuously recorded from 64 sites positioned according to the 10–20 International System, using TMS-compatible Ag/AgCl pellet electrodes mounted on an elastic cap. Additional electrodes were used as ground and reference. The ground electrode was positioned in AFz, while the reference was positioned on the tip of the nose. EEG signals were digitized at a sampling rate of 5 kHz. Skin/electrode impedance was maintained below 5 kΩ. Horizontal and vertical eye movements were detected by recording the electrooculogram to offline reject the trials with ocular artefacts.

Each TMS-EEG session consisted of single pulses (100 for T0, 80 for T1 and T2) applied at a random inter-stimulus interval (ISI) of 2 seconds with a variation of 20%. During TMS-EEG assessment subjects passive listen to a white noise and wear ear protectors to ensure the environmental noise does not affect the EEG signal. A short break was run between TMS-EEG sessions of either site. During the entire session, subjects were seated on a dedicated, comfortable armchair in a soundproofed room.

TMS-EEG Analysis

TMS–EEG data were analyzed offline with Brain Vision Analyzer (Brain Products GmbH) and EEGLAB toolbox running in a MATLAB environment (MathWorks Inc., Natick, MA). As a first step, data were segmented into epochs starting 1 s before the TMS pulse and ending 1 s after it. We first removed and then replaced data, using a cubic interpolation, from 1 ms before to 10 ms after the TMS pulse from each trial. Afterwards, data were downsampled to 1,000 Hz and bandpass filtered between 1 and 80 Hz (Butterworth zero-phase filters). A 50 Hz notch filter was applied to reduce noise from electrical sources. Then, all the epochs were visually inspected and those with excessively noisy EEG were excluded from the analysis. Independent component analysis (INFOMAX-ICA) was applied to the EEG signal to identify and remove components reflecting muscle activity, eye movements, blink-related activity, and residual TMS-related artefacts based on previously established criteria [69]. Finally, the signal was re-referenced to the average signal of all the electrodes.

To evaluate changes in cortical excitability we evaluated local cortical responses evoked by TMS. Local response was assessed, for each subject and three stimulation sites (l- DLPFC, r- DLPFC, vertex), by measuring the first six peaks (P1 from 15 to 25 ms, P2 from 26 to 47 ms, P3 from 48 to 65 ms, P4 from 66 to 75 ms, P5 from 76 to 115 ms, P6 from 116 to 145 ms) measured by the TMS-evoked potentials (TEPs) waveform at each electrode within a pooling calculated around the stimulation site (F1, F3, FC1 for l- DLPFC; F2, F4, FC2 for r- DLPFC; C1, C2, CZ for vertex).

Cortical oscillations analysis was performed using a time/frequency decomposition based on Morlet wavelet (cycles = 3; frequency resolution = 1 Hz from 4 to 50 Hz; temporal resolution = 1 ms) and then by computing TMS-related spectral perturbation (TRSP) [70,71].

To measure oscillations power and to perform the peak shifting analysis we assessed the local TRSP for each stimulated site and stimulation condition. For each TMS area, we considered a pooling computed

around the stimulation site (Same as Cortical excitability analysis, see above), and averaged the TRSP values for each of the 23 frequency layers, between 10 and 250 ms for alpha (α) and θ bands, and between 10 and 100 ms for beta (β) and γ band. These time windows were chosen considering the meantime windows of activity.

Wavelet Phase-locking value analysis is a measure of the phase synchronization of a pair of channels. It computes the randomness of the phase-locking between two channels: the index is calculated in a range between 0 and 1, where 0 represents the complete absence of phase-locking and 1 is the total phase synchronization between channels. After the computation of the wavelets and TRSP (see the paragraphs above) we applied the formula to compute the Wavelet Phase Locking Value (W-PLV) as reported in previous studies [72].

Statistical analysis

To assess the effect of iTBS + tACS stimulation on cortical excitability different repeated-measures ANOVA with within-subject factors “tACS” (γ, θ, sham) and “time” (T0, T1, T2) were performed for each site of TMS-EEG recordings. The analyses on cortical oscillations were conducted in the following steps. We first assessed the gamma oscillation at baseline (T0) in terms of frequency and power. To test if the iTBS + tACS protocol could have induced any change in the gamma band in terms of power of oscillation, we used a repeated-measures ANOVA with within-subject factors “tACS” (γ, θ, sham) and “Time” (T0, T1, T2). Then we focused on the individual frequency shifting analysis; we calculated the individual frequency peaks (the most expressed frequency in the whole oscillation spectrum) and, equally to the gamma band power analysis, we used a repeated-measures ANOVA with within-subject factors “tACS” (γ, θ, sham) and “Time” (T0, T1, T2) to assess the changes in the band’s expression in terms of shifting. For the Wavelet Phase-locking value analysis, we performed the same ANOVA analysis with different within-subject factors such as “Electrode” (F3 vs. F5; F3 vs. F4) and “Time” (T0, T1, T2).

Abbreviations

Intermittent theta burst stimulation (iTBS); Transcranial alternating current stimulation (tACS); Dorsolateral prefrontal cortex (DLPFC); TMS-evoked potential (TEPs); TMS-related spectral perturbation (TRSP); Wavelet Phase Locking Value (W-PLV).

Declarations

Funding

This research was partially supported by the Alzheimer’s Drug Discovery Foundation (ADDF), Brightfocus Foundation, and the Italian Ministry of Health to GK.

Data availability statement

Data could be requested from the corresponding author upon a rational statement.

Declaration of competing interest

None.

Author contribution statement

MM conceived the experimental setup, collected and pre-processed the data, performed the analysis and prepared the manuscript; EPC conceived the experimental setup, performed the analysis and prepared the manuscript; IB, MA, AD, VP, LC, MCP collected. pre-processed the data and performed analysis, and GK supervised the work. All authors have reviewed the manuscript.

References

1. Hanslmayr, S., Axmacher, N. & Inman, C. S. Modulating Human Memory via Entrainment of Brain Oscillations. *Trends Neurosci.* **42**, 485–499 (2019).
2. Muthukrishnan, S. P., Soni, S. & Sharma, R. Brain Networks Communicate Through Theta Oscillations to Encode High Load in a Visuospatial Working Memory Task: An EEG Connectivity Study. *Brain Topogr.* **33**, 75–85 (2020).
3. Sadaghiani, S. & Kleinschmidt, A. Brain Networks and α-Oscillations: Structural and Functional Foundations of Cognitive Control. *Trends Cogn. Sci.* **20**, 805–817 (2016).
4. Kahana, M. J. The Cognitive Correlates of Human Brain Oscillations. *J. Neurosci.* **26**, 1669–1672 (2006).
5. Mably, A. J. & Colgin, L. L. Gamma oscillations in cognitive disorders. *Curr. Opin. Neurobiol.* **52**, 182–187 (2018).
6. Benchenane, K., Tiesinga, P. H. & Battaglia, F. P. Oscillations in the prefrontal cortex: a gateway to memory and attention. *Curr. Opin. Neurobiol.* **21**, 475–485 (2011).
7. Yoon, J. H., Grandelis, A. & Maddock, R. J. Dorsolateral Prefrontal Cortex GABA Concentration in Humans Predicts Working Memory Load Processing Capacity. *J. Neurosci.* **36**, 11788–11794 (2016).
8. Barr, M. S. *et al.* Potentiation of gamma oscillatory activity through repetitive transcranial magnetic stimulation of the dorsolateral prefrontal cortex. *Neuropsychopharmacol. Off. Publ. Am. Coll. Neuropsychopharmacol.* **34**, 2359–2367 (2009).
9. Nowak, M. *et al.* Driving Human Motor Cortical Oscillations Leads to Behaviorally Relevant Changes in Local GABAA Inhibition: A tACS-TMS Study. *J. Neurosci.* **37**, 4481–4492 (2017).
10. Huang, Y.-Z., Edwards, M. J., Rounis, E., Bhatia, K. P. & Rothwell, J. C. Theta Burst Stimulation of the Human Motor Cortex. *Neuron* **45**, 201–206 (2005).
11. Larson, J., Wong, D. & Lynch, G. Patterned stimulation at the theta frequency is optimal for the induction of hippocampal long-term potentiation. *Brain Res.* **368**, 347–350 (1986).
12. Papazachariadis, O., Dante, V., Verschure, P. F. M. J., Giudice, P. D. & Ferraina, S. iTBS-Induced LTP-Like Plasticity Parallels Oscillatory Activity Changes in the Primary Sensory and Motor Areas of

Macaque Monkeys. *PLOS ONE* **9**, e112504 (2014).

13. Blumberger, D. M. *et al.* Effectiveness of theta burst versus high-frequency repetitive transcranial magnetic stimulation in patients with depression (THREE-D): a randomised non-inferiority trial. *The Lancet* **391**, 1683–1692 (2018).
14. Koch, G. *et al.* Effect of Cerebellar Stimulation on Gait and Balance Recovery in Patients With Hemiparetic Stroke: A Randomized Clinical Trial. *JAMA Neurol.* **76**, 170–178 (2019).
15. Buzsaki, G. Dendritic mechanisms of theta and ultrafast oscillations. in *European Journal of Neuroscience* vol. 10 326–326 (BLACKWELL SCIENCE LTD PO BOX 88, OSNEY MEAD, OXFORD OX2 0NE, OXON, ENGLAND, 1998).
16. Buzsáki, G. The Hippocampo-Neocortical Dialogue. *Cereb. Cortex* **6**, 81–92 (1996).
17. Wang, X.-J. & Buzsáki, G. Gamma Oscillation by Synaptic Inhibition in a Hippocampal Interneuronal Network Model. *J. Neurosci.* **16**, 6402–6413 (1996).
18. Helfrich, R. F. *et al.* Entrainment of Brain Oscillations by Transcranial Alternating Current Stimulation. *Curr. Biol.* **24**, 333–339 (2014).
19. Moisa, M., Polania, R., Grueschow, M. & Ruff, C. C. Brain Network Mechanisms Underlying Motor Enhancement by Transcranial Entrainment of Gamma Oscillations. *J. Neurosci.* **36**, 12053–12065 (2016).
20. Santarnecchi, E. *et al.* High-gamma oscillations in the motor cortex during visuo-motor coordination: A tACS interferential study. *Brain Res. Bull.* **131**, 47–54 (2017).
21. Santarnecchi, E. *et al.* Individual differences and specificity of prefrontal gamma frequency-tACS on fluid intelligence capabilities. *Cortex* **75**, 33–43 (2016).
22. Cho, R. Y., Konecky, R. O. & Carter, C. S. Impairments in frontal cortical γ synchrony and cognitive control in schizophrenia. *Proc. Natl. Acad. Sci.* <bvertical-align:super;>103</bvertical-align:super;>, 19878–19883 (2006).
23. Iaccarino, H. F. *et al.* Gamma frequency entrainment attenuates amyloid load and modifies microglia. *Nature* **540**, 230–235 (2016).
24. Chung, S. W. *et al.* Demonstration of short-term plasticity in the dorsolateral prefrontal cortex with theta burst stimulation: A TMS-EEG study. *Clin. Neurophysiol.* **128**, 1117–1126 (2017).
25. Guerra, A. *et al.* Boosting the LTP-like plasticity effect of intermittent theta-burst stimulation using gamma transcranial alternating current stimulation. *Brain Stimulat.* **11**, 734–742 (2018).
26. Guerra, A. *et al.* LTD-like plasticity of the human primary motor cortex can be reversed by γ-tACS. *Brain Stimulat.* **12**, 1490–1499 (2019).
27. Raco, V., Bauer, R., Tharsan, S. & Gharabaghi, A. Combining TMS and tACS for Closed-Loop Phase-Dependent Modulation of Corticospinal Excitability: A Feasibility Study. *Front. Cell. Neurosci.* **10**, 143 (2016).
28. Kaufman, L. D., Pratt, J., Levine, B. & Black, S. E. Antisaccades: A Probe into the Dorsolateral Prefrontal Cortex in Alzheimer's Disease. A Critical Review. *J. Alzheimers Dis.* **19**, 781–793 (2010).

29. Kikuchi, A. *et al.* Hypoperfusion in the supplementary motor area, dorsolateral prefrontal cortex and insular cortex in Parkinson's disease. *J. Neurol. Sci.* **193**, 29–36 (2001).
30. Koenigs, M. & Grafman, J. The functional neuroanatomy of depression: Distinct roles for ventromedial and dorsolateral prefrontal cortex. *Behav. Brain Res.* **201**, 239–243 (2009).
31. Weinberger, D. R., Berman, K. F. & Zec, R. F. Physiologic Dysfunction of Dorsolateral Prefrontal Cortex in Schizophrenia: I. Regional Cerebral Blood Flow Evidence. *Arch. Gen. Psychiatry* **43**, 114–124 (1986).
32. Miniussi, C. & Thut, G. Combining TMS and EEG Offers New Prospects in Cognitive Neuroscience. *Brain Topogr.* **22**, 249 (2009).
33. Casula, E. P., Pellicciari, M. C., Picazio, S., Caltagirone, C. & Koch, G. Spike-timing-dependent plasticity in the human dorso-lateral prefrontal cortex. *NeuroImage* **143**, 204–213 (2016).
34. Koch, G. *et al.* Effect of Rotigotine vs Placebo on Cognitive Functions Among Patients With Mild to Moderate Alzheimer Disease: A Randomized Clinical Trial. *JAMA Netw. Open* **3**, e2010372 (2020).
35. Hamada, M., Murase, N., Hasan, A., Balaratnam, M. & Rothwell, J. C. The Role of Interneuron Networks in Driving Human Motor Cortical Plasticity. *Cereb. Cortex* **23**, 1593–1605 (2013).
36. Hinder, M. R. *et al.* Inter- and Intra-individual Variability Following Intermittent Theta Burst Stimulation: Implications for Rehabilitation and Recovery. *Brain Stimulat.* **7**, 365–371 (2014).
37. Jannati, A., Block, G., Oberman, L. M., Rotenberg, A. & Pascual-Leone, A. Interindividual variability in response to continuous theta-burst stimulation in healthy adults. *Clin. Neurophysiol.* **128**, 2268–2278 (2017).
38. Vallence, A.-M., Kurylowicz, L. & Ridding, M. C. A comparison of neuroplastic responses to non-invasive brain stimulation protocols and motor learning in healthy adults. *Neurosci. Lett.* **549**, 151–156 (2013).
39. Huang, Y.-Z. *et al.* Plasticity induced by non-invasive transcranial brain stimulation: A position paper. *Clin. Neurophysiol.* **128**, 2318–2329 (2017).
40. Terranova, C. *et al.* Is There a Future for Non-invasive Brain Stimulation as a Therapeutic Tool? *Front. Neurol.* **9**, 1146 (2019).
41. Suppa, A. *et al.* Ten Years of Theta Burst Stimulation in Humans: Established Knowledge, Unknowns and Prospects. *Brain Stimulat.* **9**, 323–335 (2016).
42. Benali, A. *et al.* Theta-Burst Transcranial Magnetic Stimulation Alters Cortical Inhibition. *J. Neurosci.* **31**, 1193–1203 (2011).
43. Huang, Y.-Z., Rothwell, J. C., Chen, R.-S., Lu, C.-S. & Chuang, W.-L. The theoretical model of theta burst form of repetitive transcranial magnetic stimulation. *Clin. Neurophysiol.* **122**, 1011–1018 (2011).
44. Nishiyama, M., Hong, K., Mikoshiba, K., Poo, M. & Kato, K. Calcium stores regulate the polarity and input specificity of synaptic modification. *Nature* **408**, 584–588 (2000).
45. Ozen, S. *et al.* Transcranial Electric Stimulation Entrains Cortical Neuronal Populations in Rats. *J. Neurosci.* **30**, 11476–11485 (2010).

46. Gluckman, B. J. *et al.* Stochastic Resonance in a Neuronal Network from Mammalian Brain. *Phys. Rev. Lett.* **77**, 4098–4101 (1996).
47. Wiesenfeld, K. & Moss, F. Stochastic resonance and the benefits of noise: from ice ages to crayfish and SQUIDs. *Nature* **373**, 33–36 (1995).
48. Headley, D. B. & Weinberger, N. M. Gamma-Band Activation Predicts Both Associative Memory and Cortical Plasticity. *J. Neurosci.* **31**, 12748–12758 (2011).
49. Fell, J. *et al.* Human memory formation is accompanied by rhinal–hippocampal coupling and decoupling. *Nat. Neurosci.* **4**, 1259–1264 (2001).
50. Buzsáki, G. & Chrobak, J. J. Temporal structure in spatially organized neuronal ensembles: a role for interneuronal networks. *Curr. Opin. Neurobiol.* **5**, 504–510 (1995).
51. Cobb, S. R., Buhl, E. H., Halasy, K., Paulsen, O. & Somogyi, P. Synchronization of neuronal activity in hippocampus by individual GABAergic interneurons. *Nature* **378**, 75–78 (1995).
52. Fisahn, A., Pike, F. G., Buhl, E. H. & Paulsen, O. Cholinergic induction of network oscillations at 40 Hz in the hippocampus in vitro. *Nature* **394**, 186–189 (1998).
53. Tamás, G., Buhl, E. H., Lörincz, A. & Somogyi, P. Proximally targeted GABAergic synapses and gap junctions synchronize cortical interneurons. *Nat. Neurosci.* **3**, 366–371 (2000).
54. Bauer, E. P., Paz, R. & Paré, D. Gamma Oscillations Coordinate Amygdalo-Rhinal Interactions during Learning. *J. Neurosci.* **27**, 9369–9379 (2007).
55. Traub, R. D. *et al.* Gamma-frequency oscillations: a neuronal population phenomenon, regulated by synaptic and intrinsic cellular processes, and inducing synaptic plasticity. *Prog. Neurobiol.* **55**, 563–575 (1998).
56. Fries, P. A mechanism for cognitive dynamics: neuronal communication through neuronal coherence. *Trends Cogn. Sci.* **9**, 474–480 (2005).
57. Miltner, W. H. R., Braun, C., Arnold, M., Witte, H. & Taub, E. Coherence of gamma-band EEG activity as a basis for associative learning. *Nature* **397**, 434–436 (1999).
58. Montgomery, S. M. & Buzsáki, G. Gamma oscillations dynamically couple hippocampal CA3 and CA1 regions during memory task performance. *Proc. Natl. Acad. Sci.* <bvertical-align:super;>104</bvertical-align:super;>, 14495–14500 (2007).
59. Kim, K., Ekstrom, A. D. & Tandon, N. A network approach for modulating memory processes via direct and indirect brain stimulation: Toward a causal approach for the neural basis of memory. *Neurobiol. Learn. Mem.* **134**, 162–177 (2016).
60. Seeley, W. W., Crawford, R. K., Zhou, J., Miller, B. L. & Greicius, M. D. Neurodegenerative Diseases Target Large-Scale Human Brain Networks. *Neuron* **62**, 42–52 (2009).
61. Spellman, T. *et al.* Hippocampal–prefrontal input supports spatial encoding in working memory. *Nature* **522**, 309–314 (2015).
62. Sperling, R. A. *et al.* Functional Alterations in Memory Networks in Early Alzheimer's Disease. *NeuroMolecular Med.* **12**, 27–43 (2010).

63. Yamamoto, J., Suh, J., Takeuchi, D. & Tonegawa, S. Successful Execution of Working Memory Linked to Synchronized High-Frequency Gamma Oscillations. *Cell* **157**, 845–857 (2014).
64. Hosseinian, T. *et al.* External induction and stabilization of brain oscillations in the human. *Brain Stimulat.* **14**, 579–587 (2021).
65. Hosseinian, T., Yavari, F., Kuo, M.-F., Nitsche, M. A. & Jamil, A. Phase synchronized 6 Hz transcranial electric and magnetic stimulation boosts frontal theta activity and enhances working memory. *NeuroImage* **245**, 118772 (2021).
66. Zrenner, B. *et al.* Brain oscillation-synchronized stimulation of the left dorsolateral prefrontal cortex in depression using real-time EEG-triggered TMS. *Brain Stimulat.* **13**, 197–205 (2020).
67. Rothwell, J. C. Techniques and mechanisms of action of transcranial stimulation of the human motor cortex. *J. Neurosci. Methods* **74**, 113–122 (1997).
68. Rossini, P. M. *et al.* Non-invasive electrical and magnetic stimulation of the brain, spinal cord, roots and peripheral nerves: Basic principles and procedures for routine clinical and research application. An updated report from an I.F.C.N. Committee. *Clin. Neurophysiol.* **126**, 1071–1107 (2015).
69. Casula, E. P. *et al.* TMS-evoked long-lasting artefacts: A new adaptive algorithm for EEG signal correction. *Clin. Neurophysiol.* **128**, 1563–1574 (2017).
70. Casula, E. P. *et al.* Novel TMS-EEG indexes to investigate interhemispheric dynamics in humans. *Clin. Neurophysiol.* **131**, 70–77 (2020).
71. Delorme, A. & Makeig, S. EEGLAB: an open source toolbox for analysis of single-trial EEG dynamics including independent component analysis. *J. Neurosci. Methods* **134**, 9–21 (2004).
72. Chouhan, T., Robinson, N., Vinod, A. P. & Ang, K. K. Binary classification of hand movement directions from EEG using wavelet phase-locking. in 2017 *IEEE International Conference on Systems, Man, and Cybernetics (SMC)* 264–269 (2017). doi:10.1109/SMC.2017.8122613.

Figures

Figure 1

Local transcranial magnetic stimulation (TMS)-evoked cortical response of left dorsolateral prefrontal cortex (l- DLPFC). Left side graphics depict TMS-evoked activity after iTBS + γtACS stimulation (green colours), centre graphics after iTBS + θtACS stimulation (black colours) and right side graphics after iTBS + sham tACS stimulation (yellow colours). Top maps (panel (a)) represent the topographic activity within the third calculated peak (from 48 to 65 ms; -2 μV to 2 μV amplitude) in three times (from left to right respectively T0, T1, T2 time points). Panel (b) shows TMS-EEG cortical response before (T0), right after stimulation (T1), and 20 min after stimulation (T2). Panel (c) depicts histograms related to the six peaks measured by the TMS-evoked potentials (TEPs) waveform at each electrode within a pooling calculated around the stimulation site.

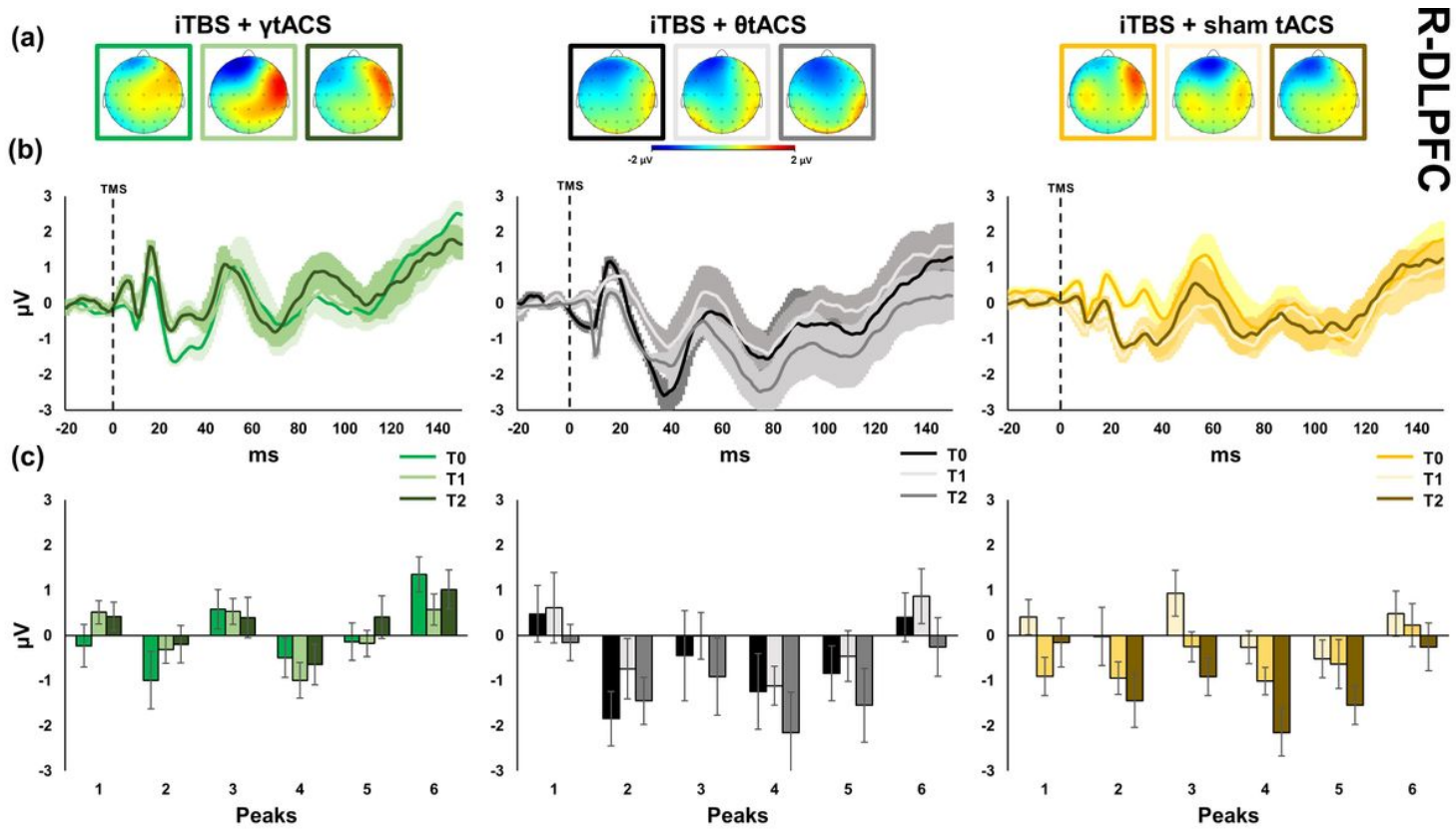

Figure 2

Local transcranial magnetic stimulation (TMS)-evoked cortical response of right dorsolateral prefrontal cortex (r- DLPFC). Left side graphics depict TMS-evoked activity after iTBS + γtACS stimulation (green colours), centre graphics after iTBS + θtACS stimulation (black colours) and right side graphics after iTBS + sham tACS stimulation (yellow colours). Top maps (panel (a)) represent the topographic activity within the third calculated peak (from 48 to 65 ms; -2 μV to 2 μV amplitude) in three times (from left to right respectively T0, T1, T2 time points). Panel (b) shows TMS-EEG cortical response before (T0), right after stimulation (T1), and 20 min after stimulation (T2). Panel (c) depicts histograms related to the six peaks measured by the TMS-evoked potentials (TEPs) waveform at each electrode within a pooling calculated around the stimulation site.

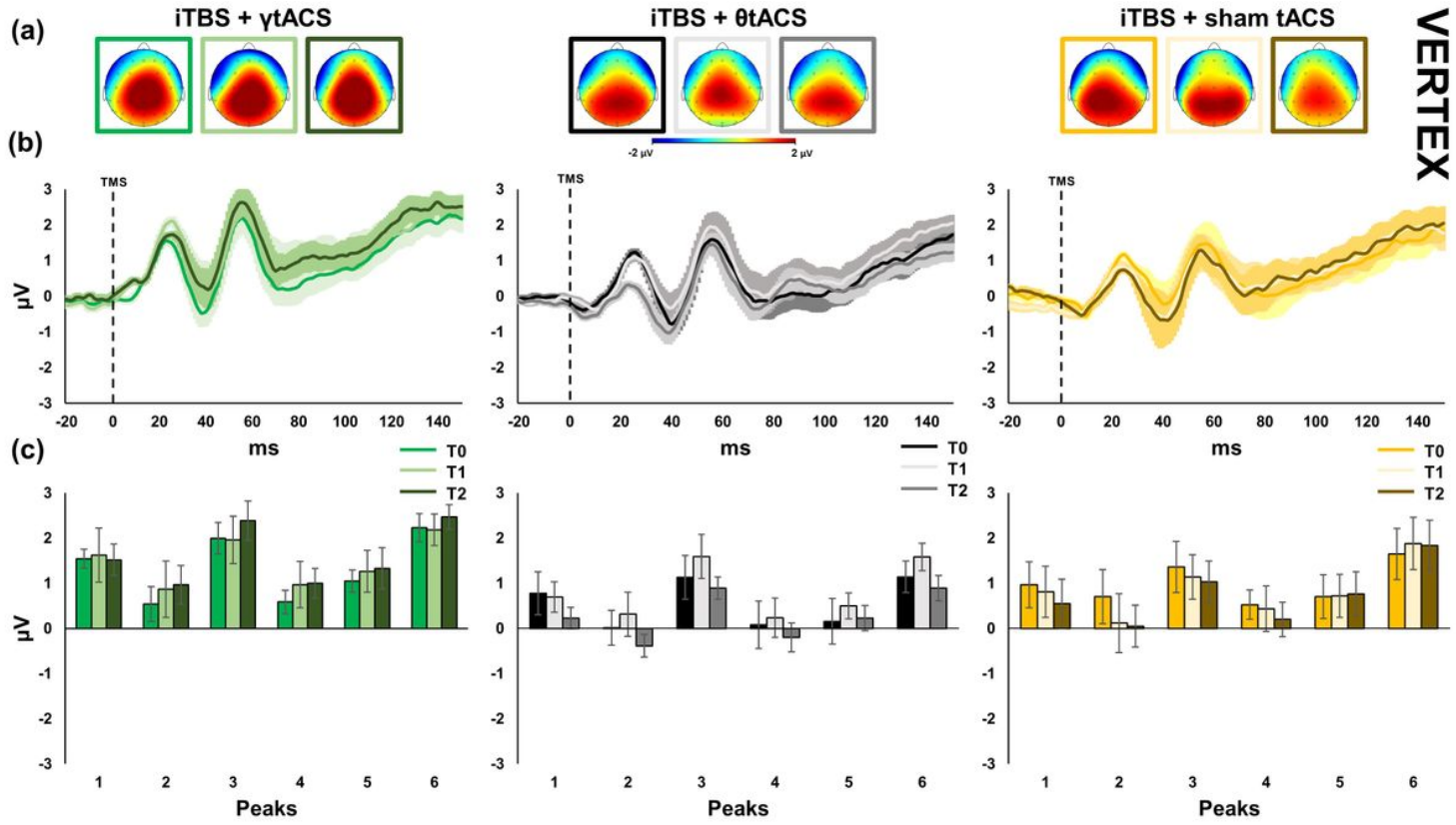

Figure 3

Local transcranial magnetic stimulation (TMS)-evoked cortical response of the vertex. Left side graphics depict TMS-evoked activity after iTBS + γtACS stimulation (green colours), centre graphics after iTBS + θtACS stimulation (black colours) and right side graphics after iTBS + sham tACS stimulation (yellow colours). Top maps (panel (a)) represent the topographic activity within the third calculated peak (from 48 to 65 ms; -2 μV to 2 μV amplitude) in three times (from left to right respectively T0, T1, T2 time points). Panel (b) shows TMS-EEG cortical response before (T0), right after stimulation (T1), and 20 min after stimulation (T2). Panel (c) depicts histograms related to the six peaks measured by the TMS-evoked potentials (TEPs) waveform at each electrode within a pooling calculated around the stimulation site.

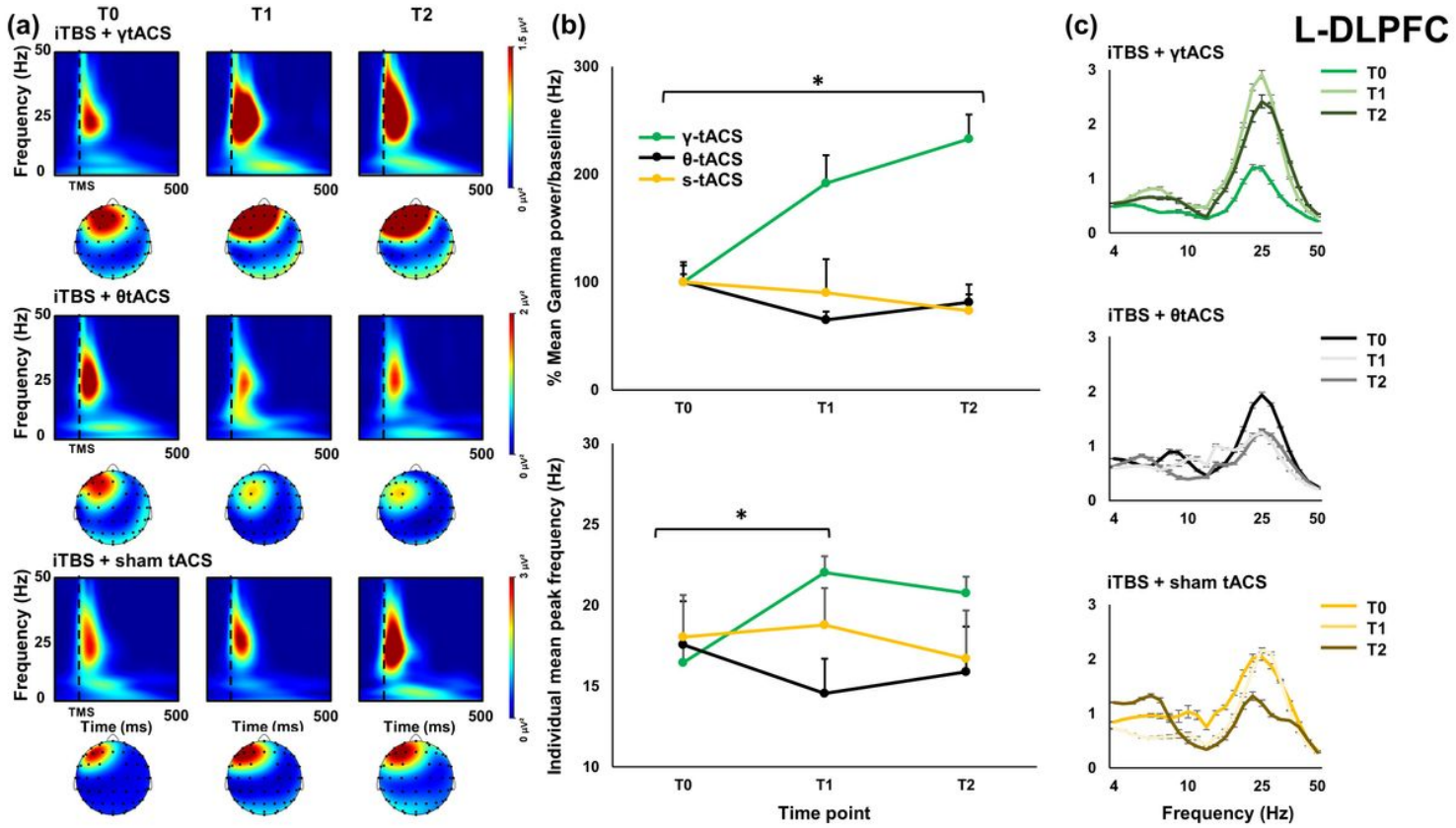

Figure 4

Local transcranial magnetic stimulation (TMS)-evoked cortical oscillations of the left dorsolateral prefrontal cortex (l- DLPFC). Panel (a) represents time-frequency oscillations for the three stimulation conditions and time points. Topographical maps depict the spatial cortical activation during TMS-EEG (50 ms after TMS pulse, 25 Hz). Panel (b) shows, on the top, the % changes of the Gamma frequency in terms of power with respect to baseline. On the bottom side is represented the shifting of the individual frequency in terms of Hz with respect to the three time points. Panel (c) depicts the individual frequency expression for the three stimulation conditions and time points.

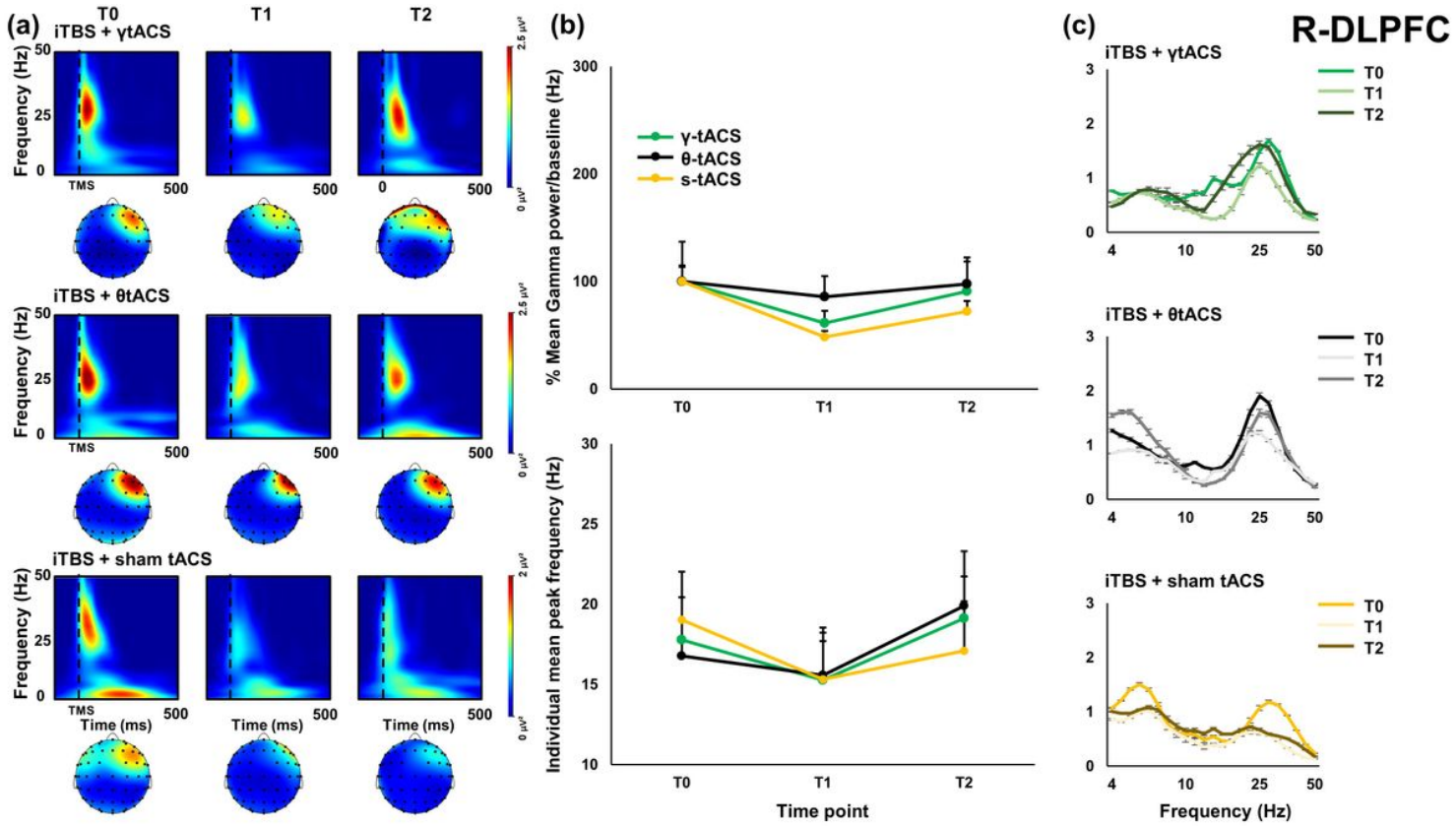

Figure 5

Local transcranial magnetic stimulation (TMS)-evoked cortical oscillations of the right dorsolateral prefrontal cortex (r- DLPFC). Panel (a) represents time-frequency oscillations for the three stimulation conditions and time points. Topographical maps depict the spatial cortical activation during TMS-EEG (50 ms after TMS pulse, 25 Hz). Panel (b) shows, on the top, the % changes of the Gamma frequency in terms of power with respect to baseline. On the bottom side is represented the shifting of the individual frequency in terms of Hz with respect to the three time points. Panel (c) depicts the individual frequency expression for the three stimulation conditions and time points.

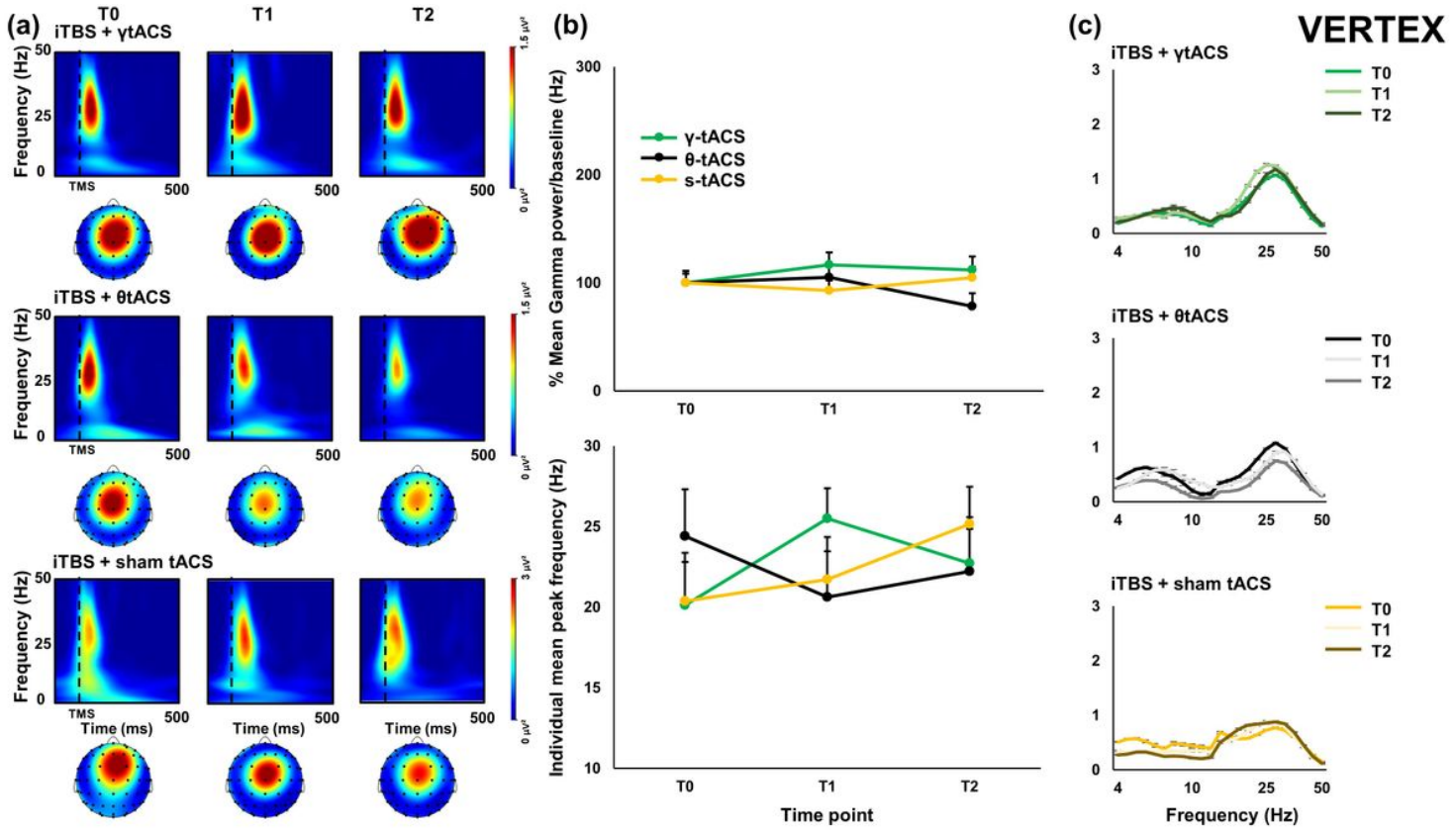

Figure 6

Local transcranial magnetic stimulation (TMS)-evoked cortical oscillations of the vertex. Panel (a) represents time-frequency oscillations for the three stimulation conditions and time points. Topographical maps depict the spatial cortical activation during TMS-EEG (50 ms after TMS pulse, 25 Hz). Panel (b) depicts the individual frequency expression for the three stimulation conditions and time points. Panel (c) shows, on the top, the changes of the 25 Hz frequency in % in terms of power with respect to baseline. On the bottom side is represented the shifting of the individual frequency in terms of Hz with respect to the three time points.

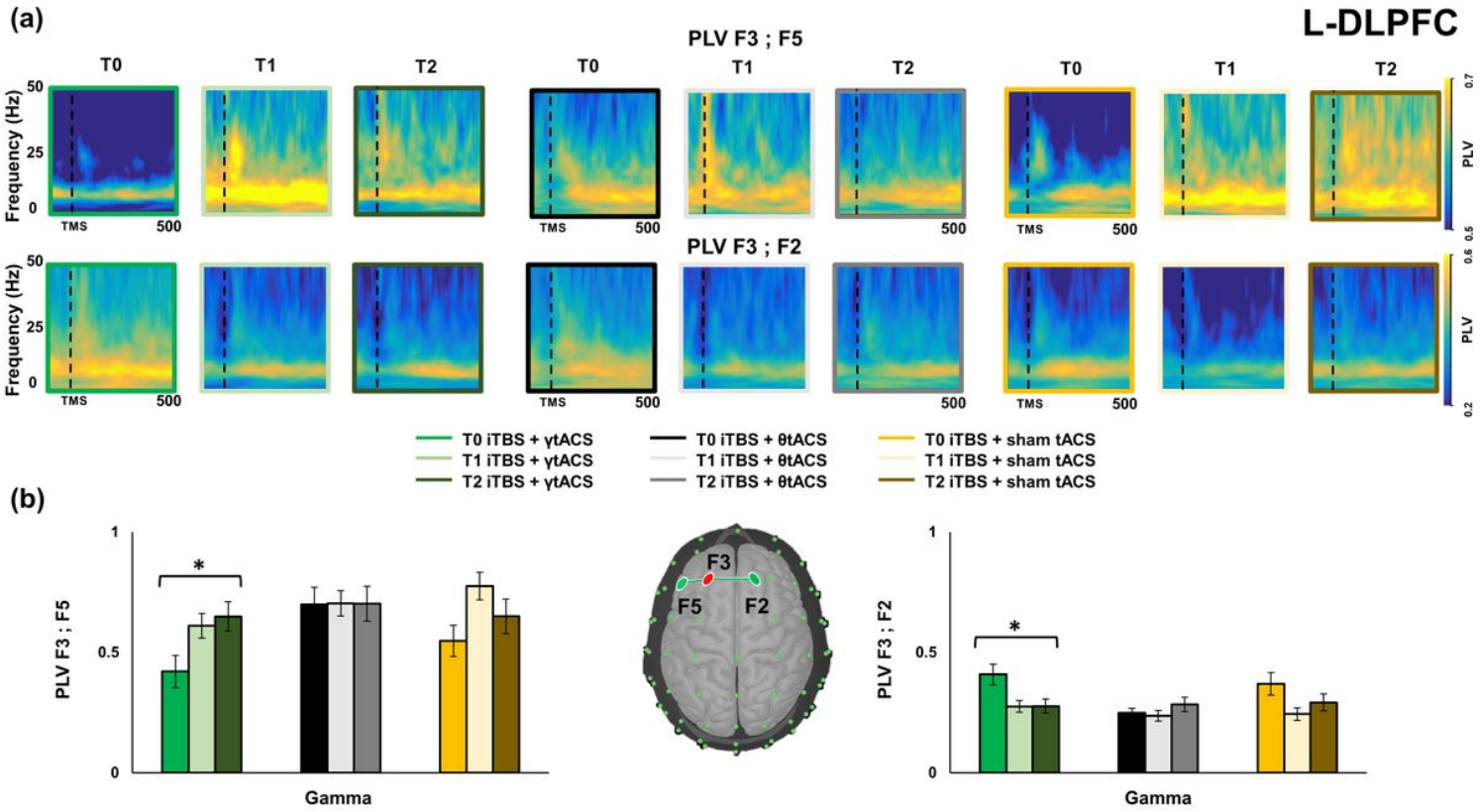

Figure 7

Paired electrodes Wavelet Phase-locking value (PLV) for the three stimulation conditions and time points on l-DLPFC. Panel (a) shows the W-PLV in a frequency (Hz) for time (ms) representation. Panel (b) shows the histograms for the 25 Hz frequency. On the centre, a topographical representation of the electrodes is coupled for the analysis.

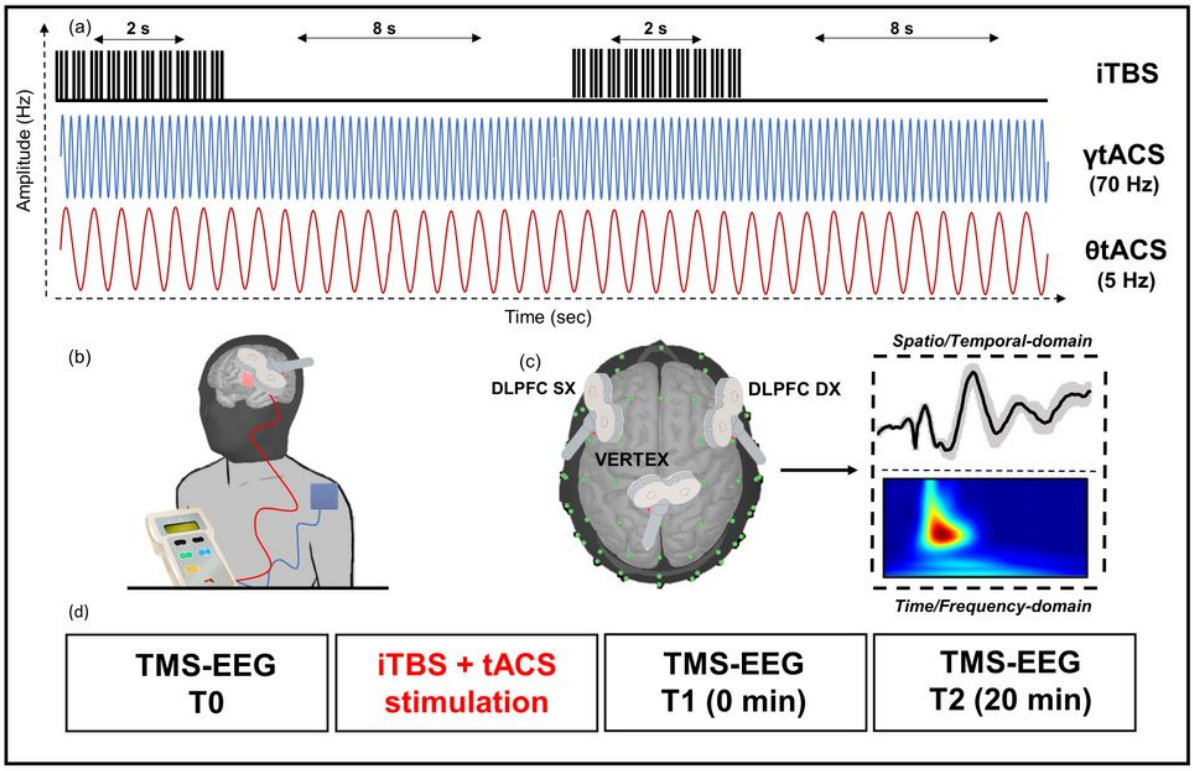

Figure 8

(a) Stimulation protocols example for intermittent theta burst stimulation (iTBS) and both gamma (γ) and theta (θ) transcranial alternated current stimulation (tACS). iTBS delivered triplets of magnetic pulses that last for 2 seconds with an interval of 10 seconds between stimulation trains; tACS delivered electrical stimulation waves at 70 Hz or 5 Hz depending on the experimental session. (b) Focus on the iTBS + tACS stimulation on dorsolateral prefrontal cortex (DLPFC). (c) Focus on the three sites stimulated to assess the effects of stimulations with TMS-EEG. (d) Experimental session design; iTBS + tACS stimulation effects were assessed before, at 0 min, and 20 after the stimulation.